SPE-195901-MS

Modeling and Optimization of Low Salinity Waterflood with Fines Transport

Seyhan Emre Gorucu, Cuong Dang, Long Nghiem, and Vijay Shrivastava, Computer Modelling Group

This paper was prepared for presentation at the SPE Annual Technical Conference and Exhibition held in Calgary, Alberta, Canada, 30 Sep - 2 October 2019.

Abstract

After nearly thirty years of research and development, it is now commonly agreed that Low Salinity Waterflood (LSW) is an attractive enhanced oil recovery (EOR) method because of its incremental oil recovery performance, reasonable operating cost and low environmental impact compared to conventional waterflood and other EOR processes. From the past studies, LSW is known as a process that comprises many mechanisms, i.e. multiple ion exchanges, wettability alteration, complex geochemical reactions, and fines migration and deposition. However, most studies in the literature have only focused on a single recovery mechanism, with varying, sometimes contradictory conclusions. This paper presents: (1) a comprehensive model that takes into account all the different important physics in LSW, i.e. fines transport, geochemistry and wettability alteration; (2) validation with a core-flood experiment; and (3) field-scale optimization of LSW.

A model for fines transport has been developed and incorporated in an Equation-of-State compositional reservoir simulator with geochemistry and wettability alteration modeling. The proposed model is capable of accounting for complex transport phenomena of fines (clay) particles in porous media including fines deposition, entrainment, and plugging. The simulator also considers physical phenomena in the oil/rock/brine system such as aqueous chemical equilibrium, rate dependent mineral reactions, multiple ion exchanges, and relative permeability alteration due to wettability changes. Validations with a LSW core-flood experiment were carried out, which provide insights into the important mechanisms for the incremental oil recovery by LSW.

The proposed model shows good agreement in terms of oil recovery and pressure drop with a benchmark LSW core-flood experiment which was conducted with a non-polar oil and in which migration of clay particles and their plugging of pores were considered as the main recovery mechanism. It is shown that the proposed model can efficiently capture the important physics in LSW processes related to fines transport. The impact of formation damage during LSW can be efficiently evaluated using this model. Finally, an optimization workflow helps maximize the recovery factor of the LSW process.

To our knowledge, this paper describes one of the first LSW mechanistic models to capture the three principal mechanisms of LSW, i.e. fines transport, geochemistry, and wettability alteration. Excellent match with laboratory experiments and field-scale optimization reinforce validity of the model. The proposed

workflow can be extended to other recovery methods such as Low-Salinity Polymer or Low-Salinity Alkali-Surfactant-Polymer.

Introduction

Several mechanisms that affect the success of LSW have been proposed (Sheng, 2014; Al-Shalabi and Sepehrnoori, 2015; Bartels *et. al.*, 2019). These mechanisms include aqueous-chemical equilibrium, rate dependent mineral reactions, multiple ion exchanges, relative permeability alteration due to wettability changes and fines transport. In this study, a fines transport model is developed that includes fines advection, deposition, entrainment and plugging equations in LSW. The fines transport model is further coupled with the aforementioned mechanisms to capture all the important physics of LSW flooding.

Tang and Morrow (1999) reported that LSW injection causes a higher pressure drop than high-salinity water (HSW) injection does. They suggested that the higher pressure drop resulted from a permeability reduction due to fines migration and plugging. During low salinity water injection, fines can be detached and entrained in water due to the change in the electrostatic and drag forces. Later on, these fines are plugged in the pore throat causing permeability reduction. Because the water initially flows through the high permeability channels, plugging occurs first in the high permeable zones. As the high permeability zones are plugged, injected water flow diverts to lower permeability zones and hence sweep efficiency improves (Sheng, 2014). The main factors that induce fines migration are water salinity, pH, velocity and temperature (Hussain *et. al.*, 2013).

Important mechanisms for fine migration are detachment/entrainment, advection, diffusion, deposition and plugging. A fine particle can be attached to or detached from the rock surface based on the electrostatic forces, gravitational forces, drag/shear force and lifting force. Electrostatic forces are London-van-der-Waals, double electric layer and born potentials. London-van-der-Waals forces are weak attraction forces between atoms and molecules due to their electromagnetic waves. Double electric layer forces are forces between charged particles. If the charge is same, the force is repulsive, and vice versa. Born repulsive forces result when the particles approach too close to one another and their electron clouds overlap. Gravitational forces occur due to the difference between the particle mass density and the water mass density. The balancing torque between these forces will determine whether the fines will be attached or detached (Civan, 2014; Bedrikovetsy *et. al.*, 2011).

There have been mixed reviews on LSW mechanisms (Hussain *et. al.*, 2013), for example, the convoluted relation between ion exchange, wettability alteration and fine migration. In order to eliminate the electrostatic effects of the oil, Yu *et. al.* (2019) used non-polar oil to isolate the effects of fine migration from ion-exchange and wettability alteration. They carried out brine injections; and two-phase oil-brine injections on two different sandstone cores: Berea and Obernkirchener. Both of the cores had quartz, kaolinite, muscovite and microcline. They observed three different mechanisms. First, kaolinite and quartz became mobile eventually causing fine plugging and fines production. Fines plugging causes permeability reduction which then causes an increasing pressure difference across the core between the inlet and the outlet. Second, they calculated the relative permeability curves based on oil breakthrough dimensionless time by using an analytical model suggested by Bedrikovetsky *et. al.* (2011). They explained that irreducible oil saturation declines due to fines retention. They also observed that only lower salinity water injection causes retention of fines whereas this is not the case for high salinity water injection. There is a balance between drag force, lifting force, gravity force and electrostatic force that determines whether or not retention occurs. A sudden reduction in salinity decreases the electrostatic force and fine particles are mobilized due to drag and lifting forces. Third, two phase injection causes higher fine production earlier. Huang et. al. (2018) and Othman et. al. (2018) concluded from those results that the interfacial tension between the two phases acting on the fine particle is another factor in fine mobilization. They were able to match their laboratory results with the permeability reduction model proposed by Pang and Sharma (1997). Similar modelling studies were carried out by Hussain *et. al.* (2013).

Several fine transport models have been postulated (Bedrikovetsky *et. al.*, 2011; Chequer *et. al.*, 2018; Yuan and Shapiro, 2011a; Yuan and Shapiro, 2011b). The equations that are used for the fine transport can also be used for other flowing solid particles/colloids such as nanomaterials, bacteria or viruses (Tufenkji, 2007). Filtration models have been developed for fines transport (Yao *et. al.,* 1971). Filtration models are based on the idea that the fines are filtrated in the pores causing plugging and hence reducing the permeability. The sink/source term for suspension/retention can be calculated as follows:

$$\frac{\partial c_{dep}}{\partial t} = k_{att} c_{flw} - k_{\det} c_{dep} \tag{1}$$

where c_{dep} and c_{flw} are retained/deposited and suspended/flowing/entrained fine concentrations, respectively. k_{att} and $k_{\det}$ are attraction and detachment coefficients, respectively. These coefficients are determined as a result of the torque balance between the electrostatic force, drag force, lifting force and gravity. Attraction and detachment terms can be a function of several parameters such as water velocity, particle diameter, temperature, salinity etc. Several expressions can be found for the attraction and detachment terms (Yao *et. al.*, 1971; Schijven and Hassanizadeh, 2000; Bedrikovetsky *et. al.*, 2011). The attraction coefficient can be expressed as,

$$k_{att} = \frac{3(1-\phi)v}{2d_c}\eta_0 \alpha \tag{2}$$

where d_c is the diameter of the collector grains. This term can be perceived as the pore diameter; ϕ is the porosity, v is the velocity, η_0 is the single-collecter contact efficiency and α is the attachment efficiency. Single collector efficiency η_0 can also be defined as the ratio of particles that strike the collector to the particles that pass the collector. α is defined as the ratio of number of collisions that succeed in adhesion to the number of collisions which occur between the suspended particles and the stabilized system (Yao *et. al.,* 1971; Tufenkji *et. al.*, 2003; Tufenkji *et. al.* 2007). Pang and Sharma (1997) express the deposition rate as a function of the concentration of suspended fines, water velocity, area of the sand grains and a trapping efficieny factor.

Bedrikovetsky *et. al.* (2009) developed a mathematical model for fine suspension, retention and flow modeling. The developed model allows the calculation of several parameters such as maximum retention concentration, filtration and formation damage coefficients. They modeled suspension-retention based on a 1D torque balance. Maximum retention concentration is a term that gives the maximum amount of fines that can be retained given a normal and drag force.

One of the most important effects of fine migration is increased pressure drop due to permeability reduction. Pang and Sharma (1997) express the permeability as

$$k_{new} = \frac{k_{old}}{1+\beta c_{dep}}. \tag{3}$$

where β is formation damage coefficient, k is permeability.

Civan (1995, 1996, 2014) express the deposition rate as

$$r_{dep} = k_d(\alpha + u) c_{flw} \phi^{2/3} \tag{4}$$

where k_d is deposition rate constant, α is stationary deposition factor, u is velocity and ϕ is porosity. Civan (2014) express plugging rate as,

$$r_{p\lg} = (k_t + k_p \phi) u c_{flw} \tag{5}$$

where k_t is the pore-throat plugging rate coefficient, k_p is the pore filling rate coefficient. Civan (2014) further expressed separate equations for entrainment due to salinity shock, velocity shock and temperature shock. For example, entrainment due to the velocity shock is a function of deposited fines, porosity and shear stress.

In the following, implementation of a new fines transport model into an equation-of-state compositional simulator (Nghiem *et. al.*, 2011) is discussed first, followed by a discussion on the geochemical processes. Model validation is done by matching the results with a laboratory test (Yu *et. al.*, 2019). A field case is then simulated and two different optimization schemes are demonstrated.

Implementation

Fines Deposition

Our implementation of the fines deposition/plugging/entrainment is an extension of the asphaltene deposition model described in Wang and Civan (2001) and Kohse and Nghiem (2004). Fines can be found in three forms as deposited (reversible), plugged (irreversible), and flowing. The material balance equation for each of the deposited fines (referred to as a fines component) is

$$\frac{\partial V_{td}}{\partial t} = \beta_{sfce} c^k_{flw} - \beta_{entr} V^k_d (v_{iw} - \beta_{vlcr}) + \beta_{plug} (1 + \beta_{snow} V^n_{td}) v_{sw} c^k_{flw} \tag{6}$$

where $V_{td} = V_d + V_p$, $V_d = V_{dep}/V_b$, $V_p = V_{p1g}/V_b$, V_{dep} is the volume of deposited fines, V_b is the volume of the gridblock, V_{p1g} is the volume of the plugged fines, c_{flw} is volumetric flowing fine concentration in water (unitless), v_{iw} is interstitial water velocity (m/day), v_{sw} is superficial water velocity (m/day), β_{sfce} is surface deposition parameter (1/day), β_{entr} is entrainment parameter (1/m), β_{vlcr} is critical velocity for entrainment (m/day), β_{plug} is plugging parameter (1/m), β_{snow} is snowball effect parameter (unitless). V_d and V_p are unitless as the volume of the fines is divided by the gridblock volume. Therefore, the unit of the equation is 1/day. cflwk is unitless because it equals the volume of flowing fine divided by volume of the aqueous phase.

In Eq. 6, the term on the left hand side is the accumulation term for both deposition and plugging. The terms on the right hand side are deposition, entrainment and plugging in order. Plugging is activated only if the minimum horizontal block permeability is less than the threshold permeability for plugging. Entrainment is activated only if the interstitial water velocity is higher than the critical velocity for entrainment (β_{vlcr}). Two important factors for fines entrainment are water velocity (drag force) and salinity (electrostatic force). Therefore, we have introduced a table where β_{vlcr} is interpolated as a function of water salinity.

Fines Advection

One dimensional material balance equation for a single fine component is

$$\frac{\partial M_{fine}}{\partial t} = \frac{\partial}{\partial x}\left(\frac{V_b \rho_w m_{flw} k_x k_{rw}}{\mu_w} \frac{\partial \Phi}{\partial x}\right) + q_{fine} \tag{7}$$

where V_b is grid block volume, k is permeability, k_{rw} is water relative permeability, ρ_w is water mass density, m_{flw} is flowing fine mass concentration in water, μ_w is viscosity, Φ is potential, q is well fine production, M_{fine} is the total amount of fines in a gridblock. The first, second and third terms are accumulation, advection and sink, respectively. It can be seen that fine components can only be transported through the aqueous phase.

Permeability Reduction and Wettability Alteration

Equation 3 shows that the permeability reduction is linearly proportional with fines plugging. Therefore, we have used resistance factor table as a function of the plugged fine concentration. The inverse of the calculated resistance factor is multiplied with the advection term in Eq. 7.

Another impact of fine migration is wettability alteration. In the case of non-polar oil, low salinity water injection can cause lower water relative permeability than high salinity water injection does. Further, low salinity water injection lowers the residual oil saturation even with the non-polar oil due to fines transport (Yu *et. al.*, 2019). Relative permeability table interpolation based on salinity, ion exchange, plugged fines, or deposited fines is used in the simulator. More information on how relative permeability interpolation is done can be found at Dang *et. al.* (2016).

Geochemical Reactions and Phase Behavior

Constraint equations are implicitly coupled with the volume balance equations while the flow equations can be implicit or explicit. Oil-gas-water phase equilibrium calculations are based on the equality of component fugacities. Water fugacity for a gaseous component that dissolves in water e.g. CO_2 can be calculated by using Henry's law (Li and Nghiem, 1986).

Chemical equilibrium calculations allow only intra-aqueous reactions and is based on $K = Q$ where K is the equilibrium constant and Q is the activity product. Mineral rate reactions are based on transition state theory (TST) (Bethke, 1996).

$$r_j = A_j k_j \left(1 - \frac{Q_j}{K_j}\right) \tag{8}$$

where j is the reaction index, r is the reaction rate and k is rate constant. Ions can be attached to the mineral surface as a balance between the ion concentration in the aqueous phase, selectivity coefficient and cation exchange capacity. The constraint equations for the for the ion exchange reactions are

$$K'_j = \prod \zeta_k \prod a_i^{v_{ji}} \tag{9}$$

$$\sum \zeta_k = 1 \tag{10}$$

where j is the reaction index, k is the ion-exchanger index, i is the ion index, K' is selectivity coefficient, a is activity, v is stoichiometric matrix, $\zeta_k = n_k|z_k|/\phi \times CEC$, n is ion-exchange mole number per unit volume, z is ion charge, ϕ is porosity and CEC is cation exchange capacity (Nghiem *et. al.*, 2011).

Incorporation of Fines into the Simulator

Throughout the simulation of LSW, fine components can be in the flowing, reversibly deposited and/or plugged form. The deposited fines are first entrained and then plugged (Fig. 1). Plugging is an irreversible process. However, initially all the specified fines are in the reversible deposited form. While fines occupy pore space and flow with the water phase, they do no affect the water phase properties directly.

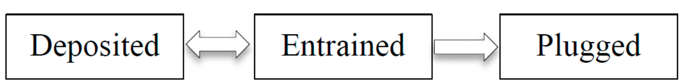

Figure 1—Fines Entrainment-Retention Modeling

Model Validation

This section presents the following. First, the proposed fines transport model is validated against LSW coreflooding experiment conducted by Yu et al. (2019). Second, LSW field-scale simulation is modelled with consideration of formation damage due to fines transport. Third, well-placement optimization is carried out for field-scale LSW with consideration of formation damage. Lastly, well-placement, injection fluid and operation conditions are optimized for field-scale LSW with consideration of formation damage due to fines transport.

Coreflooding Description and 1D Simulation Model

Yu *et. al.* (2019) performed laboratory tests only with non-polar oil in order to exclude the wettability alteration effects during low salinity brine injection. Relative permeability modification, as observed from laboratory measurements, due to fines migration and plugging was considered in the simulations performed in our work. The rock samples in this coreflood were taken from a block of outcrop Berea outcrop and had an absolute permeability of 340 md. Average porosity and pore volumes were determined gravimetrically. Core plug was 2.6 cm in diameter. Soltrol-130 non-polar oil was used. Soltrol-130 density and viscosity at 25 °C (experimental condition) are 0.755 g/l and 1.43 cp, respectively. All coreflooding experiments were performed under a constant temperature of 25 °C. Brines of various salinities were continuously injected through the core plug at a constant rate of 0.25 cm^3/min. Produced-water samples were collected for subsequent fines characterization. Salinity of the formation water is 40 g/l NaCl and the injected low salinity brine is deionized

Chemical equilibrium reactions, mineral reactions and ion-exchange reactions determine the concentration of ions and salinity. As the critical velocity for entrainment β_{vlcr} is calculated as a function of salinity, these reactions affect entrainment as well. There are two chemical equilibrium reactions, two mineral reactions and two ion-exchange reactions as shown below:

$$CO_2 + H_2O = H^+ + HCO_3^- \quad (11)$$

$$H^+ + OH^- = H_2O \quad (12)$$

$$H^+ + Calcite = Ca^{++} + HCO_3^- \quad (13)$$

$$H^+ + Magnesite = Mg^{++} + HCO_3^- \quad (14)$$

$$Na^+ + Ca - X_2 = Na - X + Ca^{++} \quad (15)$$

$$Na^+ + Mg - X_2 = Na - X + Mg^{++} \quad (16)$$

The core model is setup as one-dimensional simulation model and consists of fifty gridblocks. Yu *et. al.* (2019) provide the relative permeability tables shown in Fig. 2 for the initial reservoir conditions (high salinity) and low salinity conditions. In our model, we interpolate between these two relative permeability tables based on the amount of fine plugging.

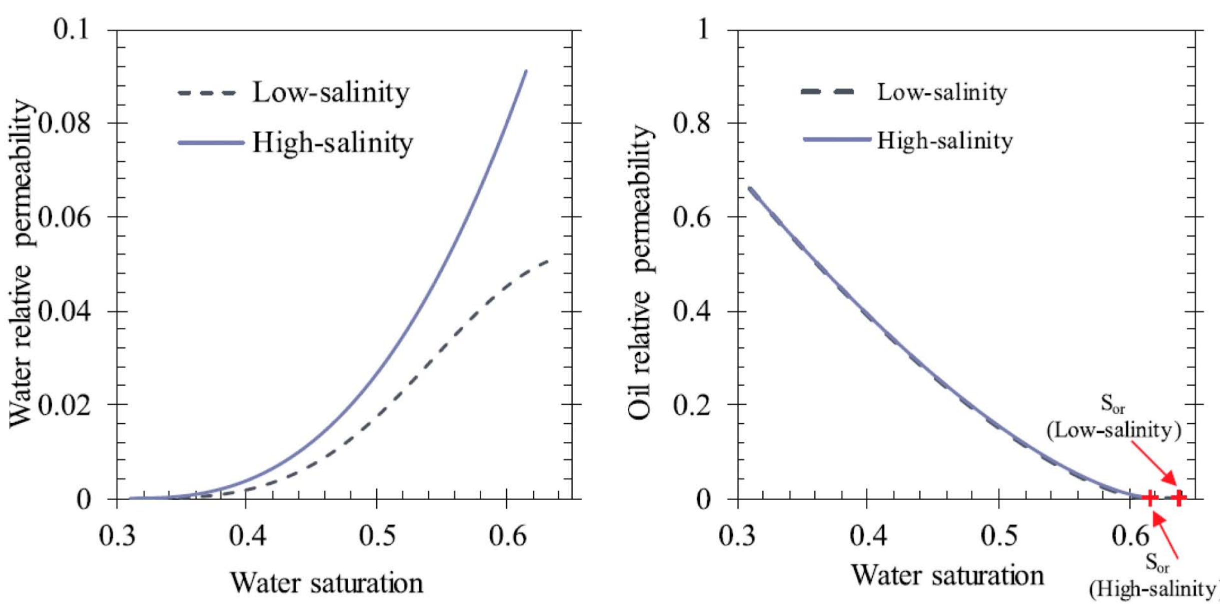

Figure 2—Relative permeability measured from lab (from Yu *et. al.*, 2019).

A history matching and optimization program was used to match the oil recovery factor and the pressure drop observed during low salinity water flooding reported at Yu *et. al.* (2019). The tuning parameters are fines related parameters i.e. resistance factor multiplier table due to plugging, salinity based critical entrainment velocity factor table, reference plugged fines (for interpolating relative permeability tables), surface deposition parameter, entrainment parameter, plugging parameter, snowball effect parameter and maximum permeability for plugging. The tuned parameters are shown in Appendix A.

Fig. 3–4 show the oil recovery factor and pressure drop between across the core for the proposed model and the lab data from Yu *et. al.* (2019). As shown, the proposed model can efficiently capture the incremental oil recovery by LSW as well as an increase in pressure drop across the core due to fines entrainment and plugging.

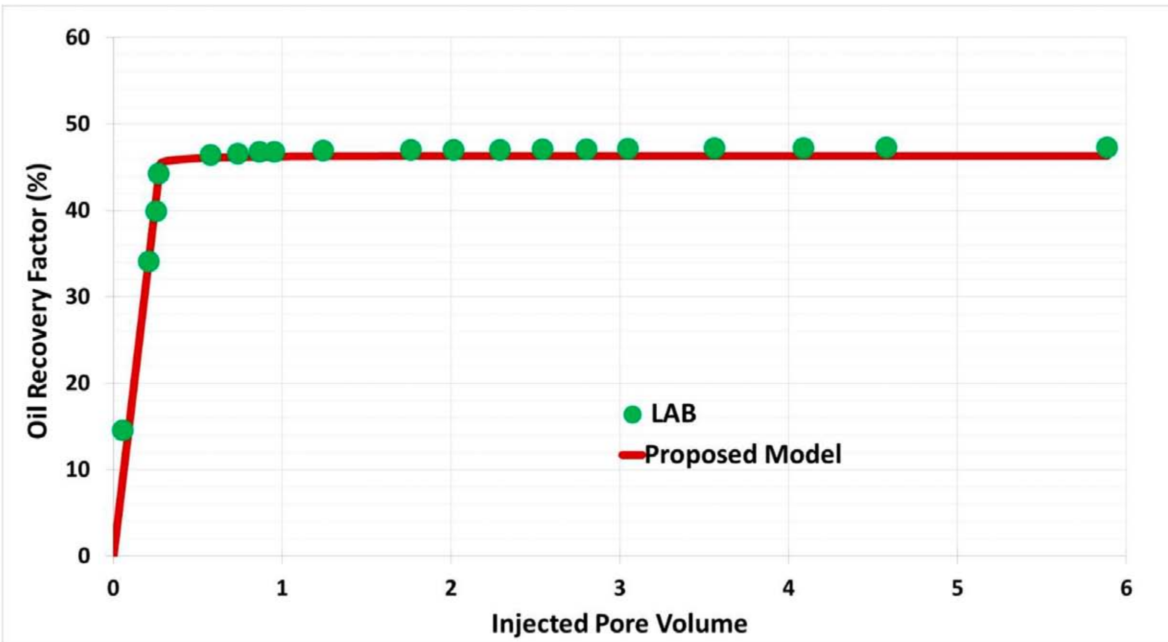

Figure 3—Oil recovery factor for the proposed model (after tuning) and the lab results from Yu *et. al.* (2019).

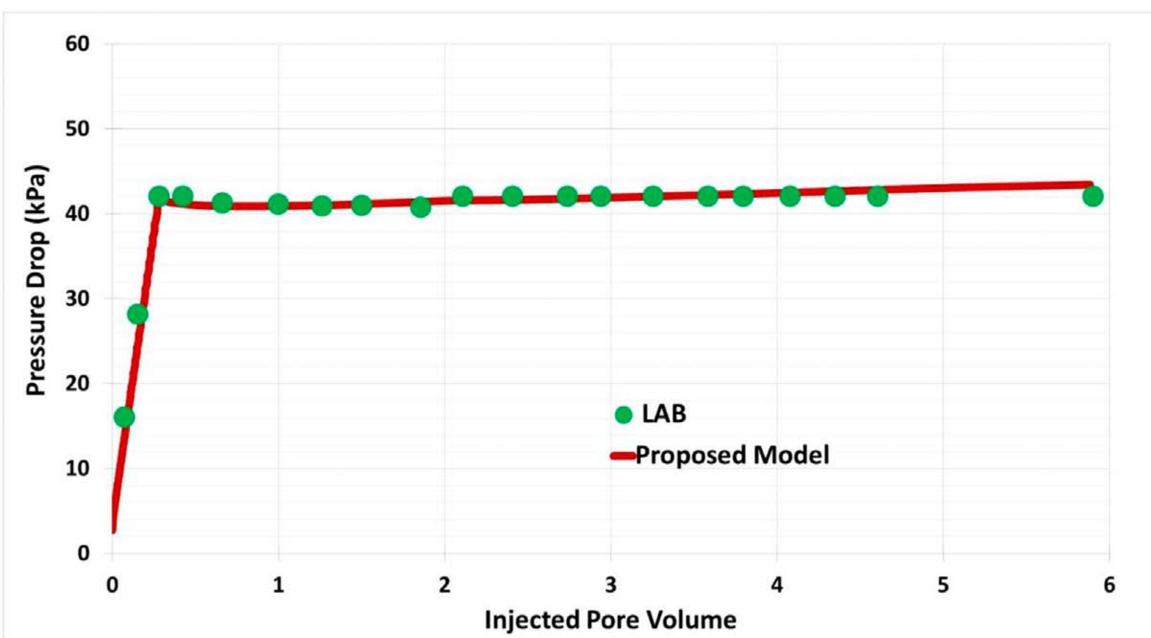

Figure 4—Pressure drop for the proposed model (after tuning) and the lab results from Yu *et. al.* (2019).

Next, a field scale LSW case is simulated with the proposed fines transport model. Injection of low salinity brine is often associated with formation damage due to fines migration and plugging. However, this phenomenon has been rarely discussed in field-scale LSW modeling. This section presents an optimization workflow for LSW with consideration of fines transport. The sandstone reservoir (shown in Fig. 5) consists of 14400 grid blocks, 9 geological layers with 3 different facies. LSW was applied in an inverted five-spot pattern. Low salinity injection causes the fines to be entrained in water and plugged around the producers as shown in Fig. 6. Fig. 7 shows that LSW injection causes higher oil recovery than conventional waterflood (HSW) does due to wettability alteration by fines migration and plugging

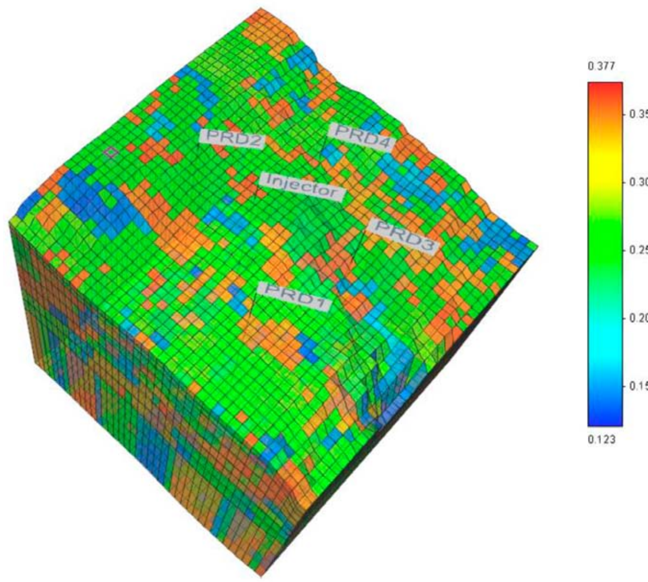

Figure 5—Porosity distribution of the field case simulation.

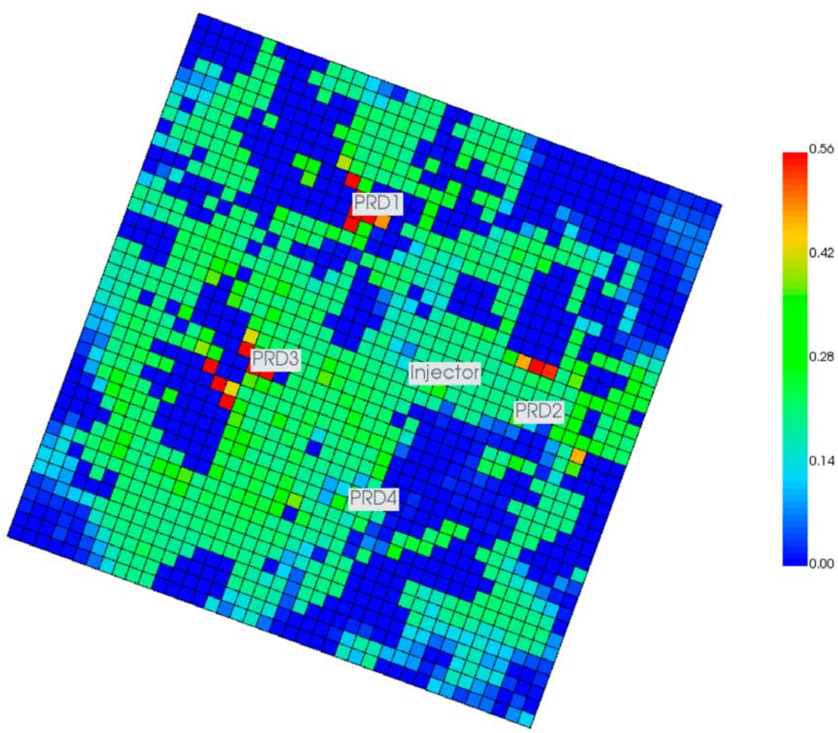

Figure 6—Volumetric concentration of plugged fines after LSW injection.

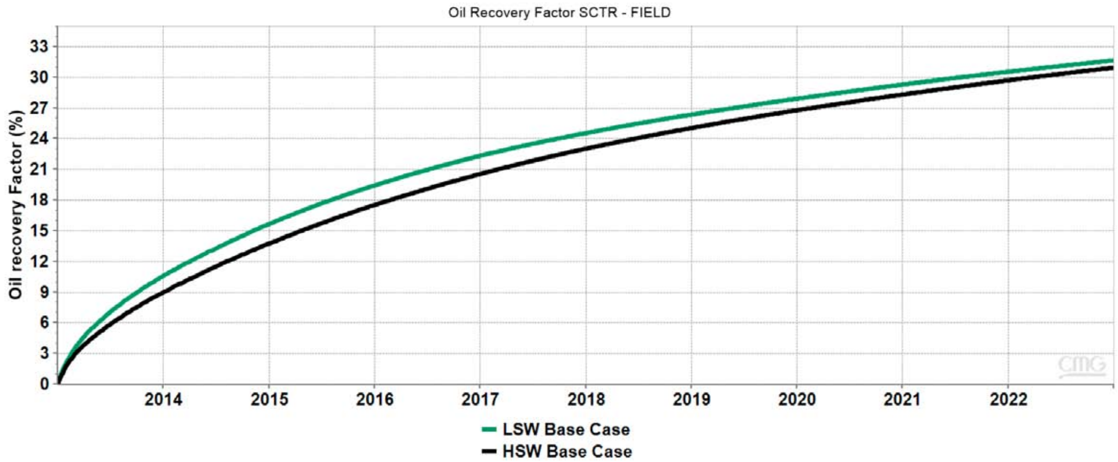

Figure 7—Oil Recovery Factor – Base Case LSW versus HSW

LSW could cause formation damage by decreasing reservoir permeability. Therefore, optimization of well-placement is important to maximize the oil recovery factor. In the first optimization case, an inverted 5-spot injection pattern was moved around the reservoir and Design Exploration and Controlled Evolution (DECE) optimization algorithm (Yang *et. al.*, 2007) was employed to find the best location for LSW implementation. Fig. 8 shows that we can significantly increase oil recovery factor by optimizing well placement in comparison with the LSW base case. The pattern was moved 140 m and 490 m in the areal x- and y-direction, respectively, compared to the base case. Fig. 9 shows the well design for the base and optimal cases.

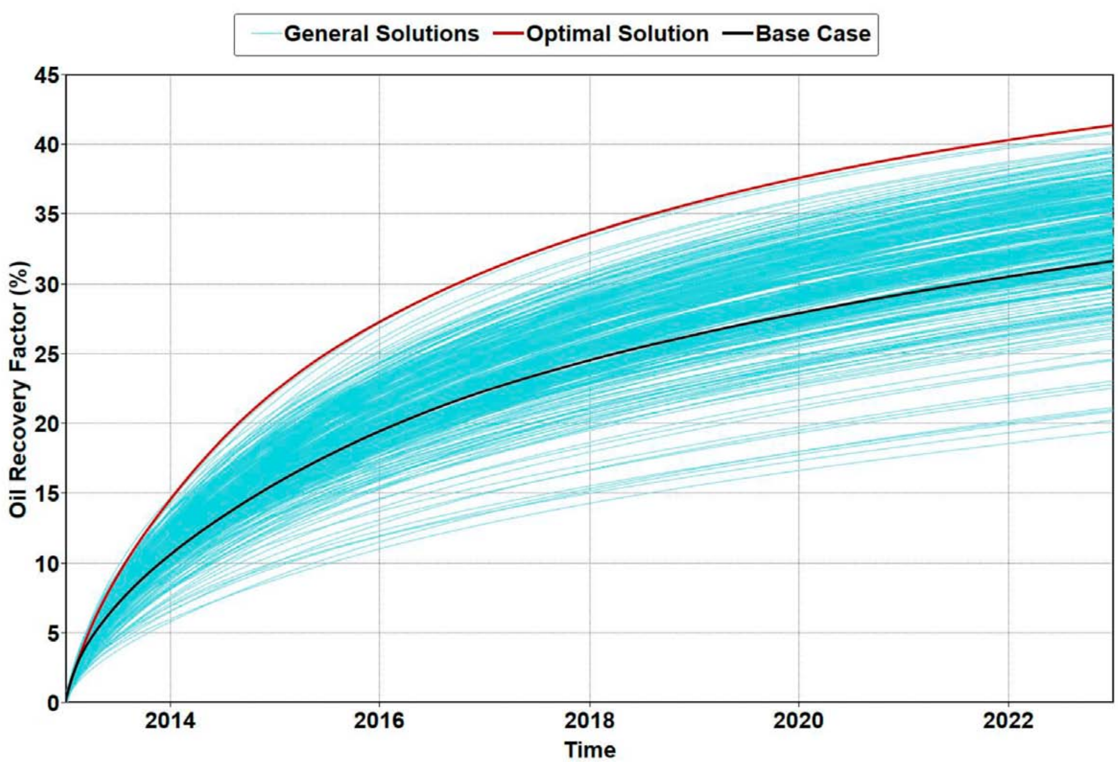

Figure 8—Oil recovery factor with different well design.

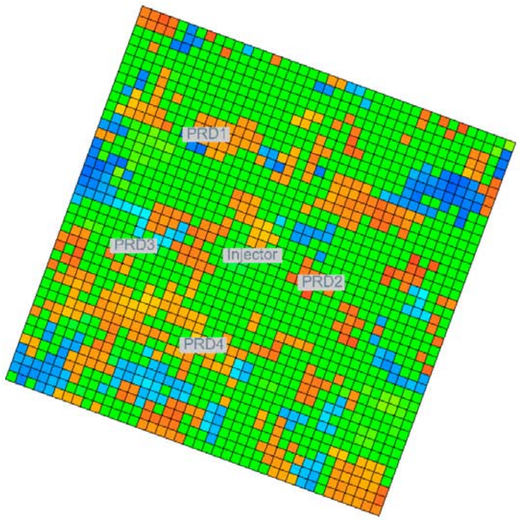

Figure 9—Well design pattern for the base case (left) and the optimum case (right).

In the second optimization case study, operating conditions and injection brine composition were optimized simultaneously along with well placement. Thirty-three optimization parameters were involved in the optimization workflow including: well-placement (x-, y-location), injection composition (Na^+, Mg^{++}, Ca^{++}), producing constrains for 4 producers every 2 years, injection rate for an injector every 2 years. Optimal solution has the same well-placement location as with the first optimization; however, oil could be produced at faster pace with higher ultimate oil recovery factor by optimizing operating conditions and the injected fluid composition. Fig. 10 shows that the second optimization study is able to increase the oil recovery by an additional 2%. Fig. 11 shows that the ultimate oil recovery is 32%, 42% and 44% for the base case, after optimization and after second optimizations, respectively.

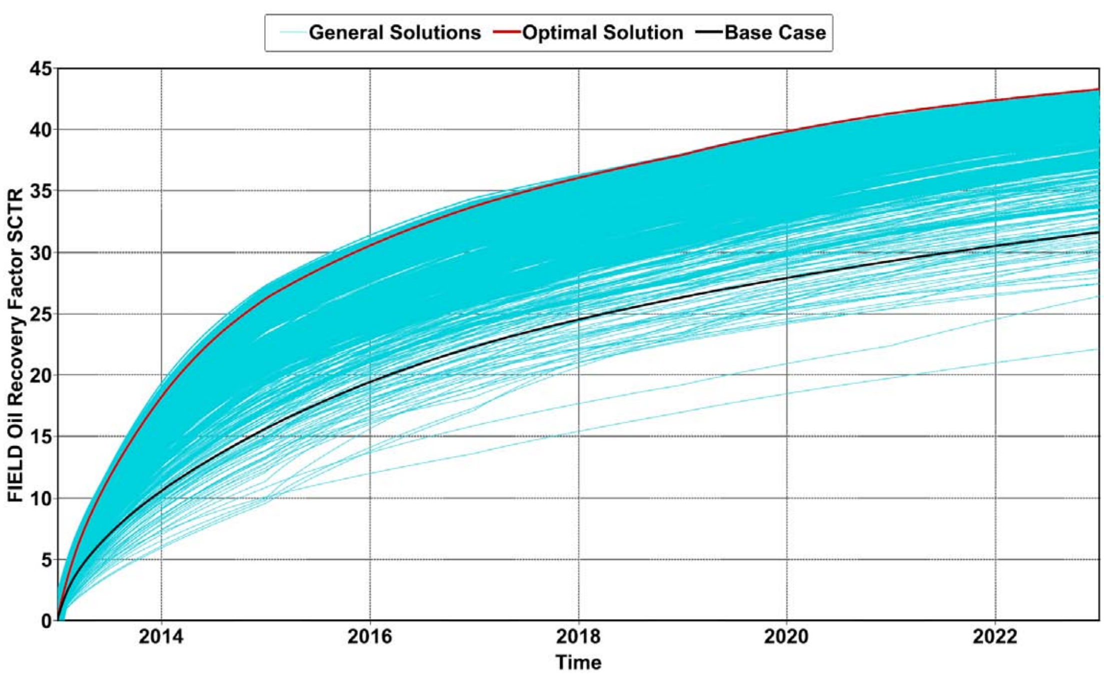

Figure 10—Optimization results for well placement and operating conditions.

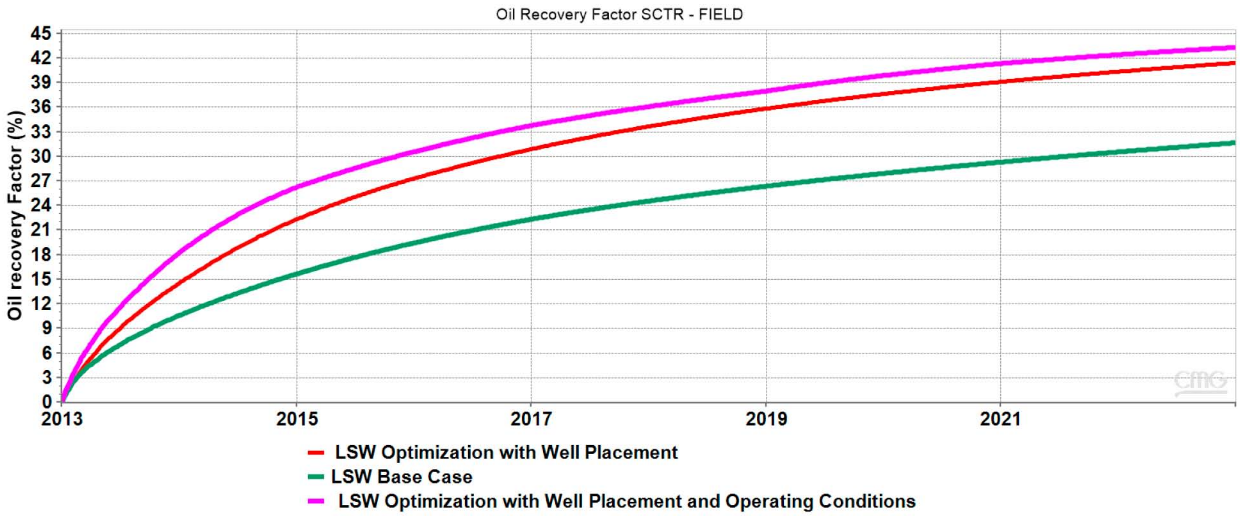

Figure 11—Oil recovery factor for the base case, after first and second optimizations.

Summary and Conclusions

Fines migration is an important aspect of oil production performance during LSW. It has been found that fines are entrained in water due to salinity and velocity. They are transported by the injected water and plug the formation. This phenomenon reduces the permeability and causes higher pressure drop. Further, formation damage due to fines may alter the relative permeability curves. In this study, a fine entrainment, deposition, plugging and advection model is implemented into an equation-of-state compositional reservoir simulator. Fines migration model was coupled with the existing chemical equilibrium reactions, mineral rate reactions and ion-exchange reactions. The proposed model efficiently matched the oil recovery factor and pressure drop by LSW conducted by Yu *et. al.* (2019). The optimization workflow presented in this paper can help to significantly increase the ultimate oil recovery.

References

Al-Shalabi, E.W. and Sepehrnoori, K. 2016. A Comprehensive Review of Low Salinity/Engineered Water Injections and Their Applications in Sandstone and Carbonate Rocks. *Journal of Petroleum Science and Engineering* **129**: 137–161.

Bartels, W.-B, Mahani, H., Berg, S., Hassanizadeh, S.M. 2019. Literature review of Low Salinity Waterflooding From a Length and Time Scale Perspective. *Fuel* **236**: 338–353.

Bedrikovetsky, P., Siqueira, F. D., Furtado, C. A., Souza, A. L. S. 2011. Modified Particle Detachment Model for Colloidal Transport in Porous Media. *Trans Porous Med* **86** (1): 353–383.

Bethke, J.M. 1996. *Geochemical Reaction Modelling*. Oxford University Press, New York, NY, USA.

Chequer, I., Vaz, A., Bedrikovetsky, P. 2018. Injectivity Decline During Low-Salinity Waterflooding Due to Fines Migration. *Journal of Petroleum Science and Engineering*. **165**: 1054–1072.

Civan, F. 1995. Modeling and Simulation of Formation Damage by Organic Deposition. In: Proceeedings of the First International Symposium on Colloid Chemistry in Oil Production: Asphaltenes and Wax Deposition, ISCOP'95, Rio de Janeiro, Brazil, November 26-29, pp. 102–107.

Civan, F. 1996. A Multi-Purpose Formation Damage Model. Proceedings of the SPE Formation Damage Symposium, Lafayette, Louisiana, February 14-15, pp. 311–326.

Civan, F. 2014. *Reservoir Formation Damage*. Gulf Professional Publishing, Burlington, MA, USA.

Dang, C. 2016. Mechanistic Modeling of Low Salinity Water Flooding. *Journal of Petroleum Science and Engineering* **146**: 191–209.

Hussain, F., Zeinijahromi, A, Bedrikovetsky, P., Badalyan, A., Carageorgos, T., Cinar, Y. 2013. An experimental Study of Improved Oil Recovery Through Fines-Assisted Waterflooding. *Journal of Petroleum Science and Engineering* **109**: 187–197.

Kohse, B. F. and Nghiem, L. X. Modelling Asphaltene Precipitation and Deposition in a Compositional Reservoir Simulator. Proceedings of the SPE/DOE Fourteenth Symposium on Improved Oil Recovery, Tusla, OK, USA, 17-21 April.

Li, Y.-K. and Nghiem, L.X. 1986. Phase Equilibria of Oil, Gas and Water/Brine Mixtures from a Cubic Equation of State and Henry's Law. *Can. J. Chem. Eng.* **64** (3): 486–496.

Nghiem, L.X., Shrivastava, V., Kohse, B. 2011. Modeling Aqueous Phase Behavior and Chemical Reactions in Compositional Simulation. Proceedings of SPE Reservoir Simulation Symposium, The Woodlands, TX, USA, 21-23 February.

Sheng, J.J. 2014. Critical Review of Low-Salinity Waterflooding. *Journal of Petroleum Science and Engineering* **120**: 216–224.

Tang, G.-Q and Morrow, N.R. 1999. Influence of brine composition and fines migration on crude oil/brine/rock interactions and oil recovery. *Journal of Petroleum Science and Engineering* **24** (2-4): 99–111

Tufenkji, N. 2007. Colloid and Microbe Migration in Granular Experiments: A Discussion of Modelling Methods. In: Frimmel F.H., Von Der Kammer F., Flemming HC. (eds) *Colloidal Transport in Porous Media*. 119–141.

Wang, S. and Civan, F. 2001. Productivity Decline of Vertical and Horizontal Wells by Asphaltene Deposition in Petroleum Reservoirs. Proceedings of SPE International Symposium on Oilfield Chemistry, Houston, TX, USA, 13-21 February.

Yang, C., Nghiem, L., Card, C., Bremeier, M. 2007. Reservoir Model Uncertainty Quantification Through Computer-Assisted History Matching. Proceedings of the SPE Annual Technical Conference and Exhibition, Anaheim, California, USA, 11-14 November.

Yao, K.-M., Habibian, M. T., O'Melia C. R. 1971. Waste and Waste Water Filtration: Concepts and Applications. *Environ Sci Technol* **5** (11): 1105–1112.

Yu, M., Zeinijahromi, A., Bedrikovetsky, P., Genolet, L., Behr, A., Kowollik, P., Hussain, F. 2019. Effects of Fines Migration on Oil Displacement by Low-Salinity Water. *Journal of Petroleum Science and Engineering* **175** (1): 665–680.

Yuan, H., Shapiro, A. A. 2011a. A Mathematical Model for Non-Monotonic Deposition Profiles in Deep Bed Filtration Systems. *Chemical Engineering Journal* **166** : 105–115.

Yuan, H., Shapiro, A. A. 2011b. Induced Migration of Fines During Waterflooding in Communicating Layer-Cake Reservoirs. *Journal of Petroleum Science and Engineering* **78** : 618–626.

Appendix A

This Appendix provides the tuned parameters that history match the oil recovery factor and pressure drop observed for Berea-2 at Yu *et. al.* (2019). Resistance factor multiplier table as a function of volumetric plugged fines concentration is shown at Table A.1. Volumetric plugged fines concentration is equal to the volume of plugged fines divided by the porous volume. Table A.2. shows critical entrainment velocity as a function of salinity. The velocity required for entrainment increases as the salinity increases. The reference value for the plugged fines –interpolation parameter used for the the oil wet table- is 0.255 kg/m^3. The reference value for the plugged fines, which is used for the water-wet table is 31.28 kg/m^3. The other fine parameters are shown below at Table A.3.

Table A.1—Volumetric Plugged Fines Concentration vs. Resistance Factor.

Volumetric Plugged Fines Concentration	**Resistance Factor**
0.0	1
1.6^{-8}	3.7

Table A.2—Salinity vs. Critical Entrainment Velocity

Salinity (Na^+ molality)	**Critical Entrainment Velocity (m/day)**
0.0	1.4^{-8}
1.73	0.0011

Table A.3—Deposition, Entrainment and Plugging Parameters for Fines.

Surface Deposition Parameter (1/day)	**91.2**
Entrainment Parameter (1/m)	36.25
Plugging Parameter (1/m)	0.063
Snowball Effect Parameter	1.445
Maximum Permeability for Plugging (mD)	340